

## THREE-AXIS ATTITUDE ESTIMATION OF SATELLITE THROUGH ONLY TWO-AXIS MAGNETOMETER OBSERVATIONS USING LKF ALGORITHM

**Mohamad Fakhari Mehrjardi, Hilmi Sanusi, Mohd. Alauddin Mohd. Ali**

National University of Malaysia (UKM), Institute of Space Science, 43600 Bangi, Malaysia  
(✉ mohamad.fakhari.m@gmail.com, +60 12 312 9908, hilmi@eng.ukm.my, mama@eng.ukm.my)

### Abstract

Estimation of satellite three-axis attitude using only one sensor data presents an interesting estimation problem. A flexible and mathematically effective filter for solving the satellite three-axis attitude estimation problem using two-axis magnetometer would be a challenging option for space missions which are suffering from other attitude sensors failure. Mostly, magnetometers are employed with other attitude sensors to resolve attitude estimation. However, by designing a computationally efficient discrete Kalman filter, full attitude estimation can profit by only two-axis magnetometer observations. The method suggested solves the problem of satellite attitude estimation using *linear Kalman filter* (LKF). Firstly, all models are generated and then the designed scenario is developed and evaluated with simulation results. The filter can achieve  $10e-3$  degree attitude accuracy or better on all three axes.

Keywords: satellite three-axis attitude estimation, two-axis magnetometer, observations, LKF, PD controller.

© 2015 Polish Academy of Sciences. All rights reserved

### 1. Introduction

Satellite attitude estimation is a problem that has been reviewed in depth over the last few decades. Since the time before Sputnik was launched in 1957, estimating the orientation of an objective in the three-dimensional space has been an interest in the field of dynamics and control. A recurrent challenge in satellite attitude estimation is to estimate the three-axis attitude from a set of noisy measurements that have been previously used or will be experienced. The estimation algorithm combines measurements in different ways to attain the required attitude estimation accuracy. In comparison with attitude determination algorithms (such as TRIAD and the Q-method), attitude estimation methods (such as the Kalman filter) are able to work with measurements of even a single attitude sensor which is an important advantage [1]. Over 50 years, the Kalman filter is still one of the most widely used data fusion systems. Typically, the Kalman filter is derived using vector algebra as a minimum mean squared estimator [2]. The Kalman filtering is most applicable for satellites equipped with three-axis gyros as well as attitude sensors [3]. Due to the power limit in satellites, processing of attitude sensor measurements by the on-board computer has computational restrictions. To solve this problem recursive algorithms based on the Kalman filter are frequently applied. The major setup issue for the Kalman filter is tuning the filter, *i.e.* precise selection of a motion model error and measurement noise statistics. Filter tuning can substantially influence the filter performance.

One of the main references on spacecraft attitude determination is by Wertz. This handbook is one of the early works used by many specialists in this field. In the field of three-axis attitude determination of a spacecraft most methods are using either a Kalman filter or batch least-squares differential correction techniques [4]. Other early attitude determination research

results have led to the TRIAD technique, the QUEST technique, and additional solutions to the Wahba's problem. Attitude determination methods based on the Wahba's loss function are generalized to include estimation of parameters other than the attitude, such as sensor noises [5–9]. Use of the Kalman filter in the Apollo navigation computer that took Neil Armstrong to the moon and (most importantly) brought him back was the most famous use of the Kalman filter in the spacecraft attitude estimation field [10]. The sensitivity of the steady-state covariance of a scalar Kalman filter to Kalman gain selection is described by Gelb [11]. Ma and Jiang have made one of the most important attempts at the magnetometer-only attitude determination. To estimate the attitude of the spacecraft and calibrate the magnetometers, they implemented an unscented Kalman filter with magnetometer measurements [12]. Mark L. Psiaki has developed and simulated three-axis magnetometer attitude determination using an extended Kalman filter. His model is proper for a low-cost three-axis attitude stabilization system beyond its usefulness purely for attitude determination. The Psiaki's Kalman filtering methods showed the error magnitude around 2–3 degrees after 100 s with a low initial filter offset [13]. Shou, H. N. and Lin C. T have developed a micro-satellite attitude determination model using Kalman filtering in a three-axis magnetometer data approach [22]. De Ruiter has presented implementation of a simple Kalman filter for correcting gyro-determined satellite attitude estimates with attitude measurements made using external sensors such as sun sensors, magnetometers, star trackers, and so on. His filter uses constant steady-state Kalman filter gains and demonstrates a close-to-optimal steady-state performance [14]. Unlike the original Monte Carlo methods [18], which used large numbers of pseudorandom samples to estimate a probability distribution, newer methods apply much smaller sample quantities for representing only the means and covariances of the distribution. Various sampling strategies have been developed for nonlinear filtering. The resulting filter implementations include sigma-point filters, [19], unscented Kalman filters [20], and particle filters [21].

The contribution of the presented research comes from addressing a problem that is very interesting in the attitude control of satellites, especially when a satellite suffers a failure in some of its attitude sensors that threatens the mission success. Every effort is to be made to save the satellite. The research at hand will answer the question: how to help the *Attitude and Orbit Determination and Control Subsystem* (AODCS) to estimate the satellite attitude using only magnetometer measurements? The objective of this work is to develop an alternative three-axis attitude estimation system using a six-state Kalman filter and only two-axis magnetometer measurements from one satellite orbit. This alternative estimation system improves the reliability of the AODCS subsystem in the absence of other attitude sensors. In this paper the application of a six-state discrete Kalman filter to estimate the satellite attitude using only noisy data from one sensor is explained.

## 2. Satellite dynamic model

The total satellite angular momentum vector consists of the angular momentum of the satellite body and the angular momentum of control actuators. The present satellite model is a three-axis attitude control satellite equipped with three reaction wheels aligned with the body frame axis. The general satellite dynamic model is given by the following expression [15]:

$$\vec{H} = \vec{H}_B + \vec{H}_W. \quad (1)$$

Transformation from one frame to another is used to simplify calculations. An appropriate attitude determination system depends on proper transformation [16]. If small angle approximations are generated and the second order terms set to be zero, the *Direction Cosine Matrix* (DCM) transformation in connexion with Euler angles and quaternions methods is easy

to employ, so they are used in this analysis. Equations of angular velocity in a rotating frame with 3→2→1 transformation are given as in [15]:

$$\omega_{BR} = \begin{bmatrix} p \\ q \\ r \end{bmatrix} = \begin{bmatrix} \dot{\phi} - \dot{\psi} \sin(\theta) \\ \dot{\theta} \cos(\phi) + \dot{\psi} \cos(\theta) \sin(\phi) \\ \dot{\psi} \cos(\phi) \cos(\theta) - \dot{\theta} \sin(\phi) \end{bmatrix}, \quad (2)$$

where:  $\omega_{BR}$  is the angular velocity vector of the body frame relative to the reference frame,  $\phi$  is the roll angle,  $\theta$  is the pitch angle,  $\psi$  is the yaw angle, and for small angles becomes:

$$\omega_{BR} = \begin{bmatrix} \dot{\phi} \\ \dot{\theta} \\ \dot{\psi} \end{bmatrix} \quad (3)$$

and

$$\omega_{BI} = \begin{bmatrix} \omega_x \\ \omega_y \\ \omega_z \end{bmatrix} = \begin{bmatrix} \dot{\phi} - \psi \Omega \\ \dot{\theta} - \Omega \\ \dot{\psi} + \phi \Omega \end{bmatrix}, \quad (4)$$

where:  $\Omega$  is the angular orbital rate of the satellite body. Based on (1), if the second order terms are neglected, the body acceleration of satellite is solved:

$$\ddot{\phi} = \left[ \frac{-4\Omega^2(I_y - I_z)\phi + \Omega h_y \dot{\phi}}{I_x} \right] + \left[ \frac{-\Omega(-I_x + I_y - I_z)\dot{\psi} + h_y \dot{\psi} - h_z \dot{\theta} + I_x \dot{\Omega} \psi}{I_x} \right] - \left[ \frac{\dot{h}_x}{I_x} \right] + \left[ \frac{T_{distx} + \Omega h_z}{I_x} \right], \quad (5)$$

$$\ddot{\theta} = \left[ \frac{-3\Omega^2(I_x - I_z)\theta - h_x \dot{\psi}}{I_y} \right] + \left[ \frac{-\Omega h_z \psi - \Omega h_x \phi + h_z \dot{\phi}}{I_y} \right] - \left[ \frac{\dot{h}_y}{I_y} \right] + \left[ \frac{T_{disty} + I_y \dot{\Omega}}{I_y} \right], \quad (6)$$

$$\ddot{\psi} = \left[ \frac{-\Omega^2(-I_x + I_y)\psi + \Omega h_y \dot{\psi}}{I_z} \right] + \left[ \frac{-\Omega(I_x - I_y + I_z)\dot{\phi} + h_x \dot{\theta} - h_y \dot{\phi} - I_z \dot{\Omega} \phi}{I_z} \right] - \left[ \frac{\dot{h}_z}{I_z} \right] + \left[ \frac{T_{distz} - \Omega h_z}{I_z} \right], \quad (7)$$

where:  $T_{dist}$  is the disturbance torque vector.

By the following state variable substitutions these second order equations are reduced to the first order equations:

$$\vec{x} = \begin{bmatrix} \phi & \dot{\phi} & \theta & \dot{\theta} & \psi & \dot{\psi} \end{bmatrix}^T. \quad (8)$$

With this replacement, the satellite dynamic equations are expressed in the matrix form:

$$\dot{\vec{x}} = (A - BF)x + Bu_d. \quad (9)$$

A is the plant matrix given by:

$$A = \begin{bmatrix} 0 & \frac{-4\Omega^2(I_y - I_z) + \Omega h_y}{I_x} & 0 & \frac{-\Omega h_y}{I_y} & 0 & -\dot{\Omega} \\ 1 & 0 & 0 & \frac{-h_z}{I_y} & 0 & \frac{-\Omega(I_x - I_y + I_z) - h_y}{I_z} \\ 0 & 0 & 0 & \frac{-3\Omega^2(I_x - I_z)}{I_y} & 0 & 0 \\ 0 & \frac{-h_z}{I_x} & 1 & 0 & 0 & \frac{h_x}{I_z} \\ 0 & \dot{\Omega} & 0 & \frac{-\Omega h_z}{I_y} & 0 & \frac{-\Omega^2(-I_x + I_y) + \Omega h_y}{I_z} \\ 0 & \frac{-\Omega(I_x - I_y + I_z) - h_y}{I_x} & 0 & \frac{-h_x}{I_y} & 1 & 0 \end{bmatrix}, \quad (10)$$

B is the control matrix given by:

$$B = \begin{bmatrix} 0 & 1 & 0 & 0 & 0 & 0 \\ 0 & 0 & 0 & 1 & 0 & 0 \\ 0 & 0 & 0 & 0 & 0 & 1 \end{bmatrix}^T. \quad (11)$$

F is the *proportional derivative* (PD) controller gain matrix and  $u_d$  is the matrix of disturbance moments and internal reaction wheel moments:

$$F = \begin{bmatrix} \frac{k_x}{I_x} & \frac{k_{vx}}{I_x} & 0 & 0 & 0 & 0 \\ 0 & 0 & \frac{k_y}{I_y} & \frac{k_{vy}}{I_y} & 0 & 0 \\ 0 & 0 & 0 & 0 & \frac{k_z}{I_z} & \frac{k_{vz}}{I_z} \end{bmatrix}, \quad (12)$$

$$u_d = \begin{bmatrix} \frac{T_{distx} + \Omega h_z}{I_x} & \frac{T_{disty} + I_y \dot{\Omega}}{I_y} & \frac{T_{distz} - \Omega h_x}{I_z} \end{bmatrix}^T. \quad (13)$$

### 3. Magnetometer model

A magnetometer sensor is chosen because of its reasonable accuracy, mass and power consumption. A magnetometer provides an accurate value for the magnetic field vector at

the location of the satellite. This sensor measures the direction and magnitude of the local geomagnetic field in the orbit. Comparing magnetometer measurements with the same vector in the inertial frame determines the attitude of satellite. The measurement model is assumed to be of the form given by:

$$\tilde{B}_B = AB_I + v, \tag{14}$$

where:  $\tilde{B}_B \in R^3$  is the magnetic field measurement in the satellite body coordinate system,  $A \in R^3$  is the transformation matrix that maps the inertial frame to the body frame,  $B_I \in R^3$  is the known magnetic field vector in inertial coordinates, and  $v$  is assumed to be the zero-mean Gaussian measurement error with the standard deviation  $\sigma_m I_{3 \times 3}$ . In this simulation, axes of the magnetometer are aligned with the body axes. At each discrete time step data from tow magnetometer axes are selected at random for attitude determination. For the purpose of this study, it is assumed that the measurement error of the magnetometer is regulated as if the accuracy of the sensor was less than  $0.1^0$ . The noise level is inherent to the magnetometer and is treated as a zero-mean Gaussian white sequence. Also, the magnetometer sampling rate is considered to be 0.1 Hz.

The model used by the attitude determination system is the World Magnetic Model that has been discussed in [23]. The World Magnetic Model uses spherical harmonics to calculate the Earth’s magnetic field vector at any point in space over time. The model requires the current position and time of the satellite to quantify the magnetic field vector. The magnetic field vector of the Earth can be returned at any point of the orbit by the given position. The magnetic field model used in this study takes the form:

$$B(\lambda, \varphi, r, t) = -\Delta V(\lambda, \varphi, r, t), \tag{15}$$

where:

$$\Delta V(\lambda, \varphi, r, t) = a \left\{ \sum_{n=1}^N \sum_{m=0}^n (g_n^m(t) \cos(m\lambda) + h_n^m(t) \sin(m\lambda)) \left(\frac{a}{r}\right)^{n+1} P_n^m(\sin \varphi) \right\} \tag{16}$$

and  $\lambda$ ,  $\varphi$ , and  $r$  are the longitude, latitude, and radial distance to the centre of Earth, respectively. And:

$$P_n^m(v) = \begin{cases} \sqrt{2 \frac{(n-m)!}{(n+m)!}} P_{n,m}(v) & \text{if } m > 2, \\ P_{n,m}(v) & \text{if } m = 0, \end{cases} \tag{17}$$

where the parameters  $g$  and  $h$  in (16) are available in a tabular format in the World Magnetic Model and the parameter  $a$  is the geomagnetic reference radius.

#### 4. Kalman filter design

In the field of satellite attitude estimation, the family of Kalman filter algorithms estimate the state of a satellite system basing on recursive noisy measurements, and minimize the cost function which is given by:

$$J = E[(\hat{X}_k - X_k)^T (\hat{X}_k - X_k)], \tag{18}$$

where:  $E$  is the expectation,  $X_k$  is the true plant state vector, and  $\hat{X}_k$  is the estimated state vector [1]. The discrete Kalman filter structure given in [17] is based on:

$$\begin{aligned}
 \hat{x}_k &= \hat{x}_k^- + K_k (z_k - H_k \hat{x}_k^-), \\
 K_k &= \bar{P}_k H_k^T (H_k \bar{P}_k H_k^T + R_k)^{-1}, \\
 P_k &= (I - K_k H_k) P_k^-, \\
 \hat{x}_{k+1}^- &= \varphi_k \hat{x}_k, \\
 P_{k+1}^- &= \varphi_k P_k \varphi_k^T + Q_k
 \end{aligned} \tag{19}$$

and Table 1 shows the filter definitions.

Table 1. Kalman filter definitions.

Symbol	Definition	Size	Symbol	Definition	Size
$\bar{x}_k$	State vector	$6 \times 1$	$H_k$	Feedback sensitivity matrix	$3 \times 6$
$\Phi_k$	State transition matrix	$6 \times 6$	$\bar{v}_k$	Sensor white noise sequence	$3 \times 1$
$\Delta_k$	Deterministic weighting matrix	$6 \times 3$	$R_k$	Sensor noise covariance matrix	$3 \times 3$
$\bar{u}_k$	Deterministic forcing function	$3 \times 1$	$P_k$	Error covariance matrix	$6 \times 6$
$\bar{w}_k$	Plant white noise sequence	$6 \times 1$	$\hat{x}_k$	Optimal estimate of $\bar{x}_k$	$6 \times 1$
$Q_k$	Plant noise covariance matrix	$6 \times 6$	$\hat{x}_k^-$	Estimate of state $\bar{x}_k$ at time prior	$6 \times 1$
$\bar{z}_k$	Measurement vector	$3 \times 1$	$K_k$	Optimal Kalman gain	$6 \times 3$

The filter itself is based on a prediction process which is followed by an update process. In this work, before updating the covariance prediction, first the Kalman Gain with the initial covariance prediction is calculated and then a new prediction is generated.

A six-state linear Kalman filter has been chosen to estimate both attitude and attitude rates from the noisy magnetometer data. A favourable characteristic of this recursive filter is that there is no need to store previous sensor measurements. The value of the optimal Kalman gain matrix varies with each time step. In the implementation of the discrete Kalman filter, the measurement noise covariance is usually practically measured prior to operation of the filter. Defining the plant noise covariance is generally more challenging because we typically are unable to directly observe the process we are estimating. In this work, the plant noise covariance matrix is varying with time and the solution for extracting the plant noise covariance matrix given by [17] is used.

First the matrix  $\beta$  is formed:

$$\beta = \expm \left( \begin{bmatrix} -A & BWB^T \\ 0 & B^T \end{bmatrix} \Delta t \right) = \begin{bmatrix} \dots & \phi^{-1} Q_k \\ 0 & \phi^T \end{bmatrix}, \tag{20}$$

where:  $W$  is the power spectral density matrix associated with the forcing function  $u_d$ . To get  $\Phi$ , the lower-right partition of  $\beta$  is transposed and then the  $Q$  is obtained from the upper-right partition of  $\beta$ . For the purpose of analysis and proper tuning, the time varying nature of  $Q$  matrix over one period of orbit is considered.

To enter the Kalman filter loop, an initial estimate,  $\hat{x}_0^-$ , and its error covariance,  $P_0^-$ , are chosen:

$$\hat{x}_0^- = \begin{bmatrix} 0 \\ 0 \\ 0 \\ 0 \\ 0 \\ 0 \end{bmatrix}, \tag{21}$$

$$P_0^- = 10^{-12} \begin{bmatrix} 1 & 0 & 0 & 0 & 0 & 0 \\ 0 & 1 & 0 & 0 & 0 & 0 \\ 0 & 0 & 1 & 0 & 0 & 0 \\ 0 & 0 & 0 & 1 & 0 & 0 \\ 0 & 0 & 0 & 0 & 1 & 0 \\ 0 & 0 & 0 & 0 & 0 & 1 \end{bmatrix}, \tag{22}$$

where the ‘^’ superscript presents estimation while the ‘-’ notation denotes estimation.

During the simulation by taking a closer look at the filter it was proved that some system covariance matrix variables can be adjusted to modify the filter performance. The system covariance matrix is an assumption of noise which occurs in the system model. Because a small system covariance matrix correlates to small amount of noise and has naturally a better estimate result, therefore it is evident that the desired system covariance matrix should be the smallest possible.

For the purpose of proper tuning of the filter, considering the time varying nature of both *Q* and *P* matrices is essential. In the simulation, if *Q* decreases, the filter will have a tendency to follow the predicted estimate. On the other hand, if *Q* increases, the filter will follow the measurements. So a right balance has been found for the filter because if *Q* is too low, then the filter has difficulty in tracking satellite manoeuvres, but if *Q* is too high, the pointing accuracy suffers from the magnetometer noise effect.

### 5. Proportional plus derivative controller

Many types of controllers are available and each of them has its own unique characteristics. It is shown that gains of a PD controller can be adjusted to minimize the settling time and overshoot. Each reaction wheel is equipped with a separate PD controller. The following PD controllers are used for three reaction wheels and they are given by [15]:

$$\begin{aligned} \dot{h}_x &= k_{vx} \dot{\phi} + k_x \phi, \\ \dot{h}_y &= k_{vy} \dot{\theta} + k_y \theta, \\ \dot{h}_z &= k_{vz} \dot{\psi} + k_z \psi. \end{aligned} \tag{23}$$

These control laws are based on the change rate of reaction wheel angular momentum that is the reaction wheel torque and are a function of the measured Euler angles and rates. Determination of suitable position and rate feedback gains is necessary to obtain robustness.

The following equation is used to determine the Euler moment relations [15]:

$$\vec{T} = \frac{d}{dt}(\vec{H}_I) = \frac{d}{dt}(\vec{H}_B) + \omega \times \vec{H}, \tag{24}$$

where:  $\vec{T}$  is the total torque vector,  $\vec{H}_I$  is the angular momentum of the satellite with respect to the inertia frame,  $\vec{H}_B$  is the angular momentum of the satellite around the body frame and  $\omega$  is the satellite angular velocity. It is assumed that the second order terms are neglected and it can be shown that the equations are [15]:

$$\begin{aligned} T_x &= I_x \ddot{\phi} + 4\Omega^2(I_y - I_x)\phi - \Omega h_y \dot{\phi} - \Omega h_z + \Omega(-I_x + I_y - I_z)\dot{\psi} - h_y \dot{\psi} + h_z \dot{\theta} - I_x \dot{\Omega} \psi + \dot{h}_x, \\ T_y &= I_y \ddot{\theta} + 3\Omega^2(I_x - I_z)\theta + h_x \dot{\psi} + \Omega h_z \psi + \Omega h_x \dot{\phi} - h_z \dot{\phi} - I_y \dot{\Omega} + \dot{h}_y, \end{aligned} \tag{25}$$

$$T_z = I_z \ddot{\psi} + \Omega^2(-I_x + I_y)\psi - \Omega h_y \psi + \Omega h_x + \Omega(I_x - I_y + I_x)\dot{\phi} - h_x \dot{\theta} + h_y \dot{\phi} + I_z \dot{\Omega} \phi + \dot{h}_z.$$

These equations describe the motion of the satellite when subject to external torques. By decoupling and taking the transform function of equations the following results are obtained:

$$\begin{aligned} \frac{\phi(s)}{T_x(s)} &= \frac{\frac{1}{I_x}}{s^2 + \frac{k_{vx}}{I_x}s + \frac{4\Omega^2(I_y - I_x) - \Omega h_y + k_x}{I_x}}, \\ \frac{\theta(s)}{T_y(s)} &= \frac{\frac{1}{I_y}}{s^2 + \frac{k_{vy}}{I_y}s + \frac{3\Omega^2(I_x - I_z) + k_y}{I_y}}, \\ \frac{\psi(s)}{T_z(s)} &= \frac{\frac{1}{I_z}}{s^2 + \frac{k_{vz}}{I_z}s + \frac{\Omega^2(-I_x + I_y) - \Omega h_y + k_z}{I_z}}. \end{aligned} \tag{26}$$

The objective is to determine suitable position and feedback gains to increase satellite robustness. The nominal characteristic equation for the second order system and the final value theorem [24] are used to determine the feedback gains:

$$\Lambda(s) = s^2 + 2\omega_n \xi s + \omega_n^2, \tag{27}$$

$$f(\infty) = \lim_{t \rightarrow \infty} f(t) = \lim_{s \rightarrow 0} sF(s), \tag{28}$$

where:  $\omega_n$  is the natural frequency, and the damping factor is denoted  $\xi$ . Each of the denominators in (26) is inserted to (27). By applying these equations the position feedback gains are determined from the following equations:

$$\begin{aligned} k_x &= \frac{T_x - 4\Omega^2(I_y - I_x)\phi_{ss} + \Omega h_y \phi_{ss}}{\phi_{ss}}, \\ k_z &= \frac{T_z - \Omega^2(-I_x + I_y)\psi_{ss} + \Omega h_y \psi_{ss}}{\psi_{ss}}, \end{aligned} \tag{29}$$

where: *ss* subscript denotes the steady state.

The natural frequency is determined by taking the square root of the last term in denominator in (26). After that, the velocity feedback gains are calculated:

$$\begin{aligned}k_{vx} &= 2\omega_{nx}I_x, \\k_{vy} &= 2\omega_{ny}I_y, \\k_{vz} &= 2\omega_{nz}I_z.\end{aligned}\tag{30}$$

## 6. Simulation testing

An important complement in analysing Kalman filter evaluation is simulation testing. The code is started by defining some known constants, and then defining the number of time steps and the duration of each time step. The simulation is run for one orbital period which is sufficient to evaluate how fine the filter is following changes in the trajectory. Systematic errors such as a parameter uncertainty or biases mostly reduce the stability or accuracy, or both. The simulation combines the satellite attitude dynamics equation with a definite initial state  $x(t_0)$  to generate the state time history  $x(t_k)$  for  $k=0,1,2,\dots$ . The filter takes noisy measurements and integrates with the initial estimate of covariance and estimates of the initial states to produce an estimate of the state time history  $\hat{x}^+(t_k)$  for  $k=0,1,2,\dots$ . Even with disturbance torques, measurement noise and a modelling error, the estimated state  $\hat{x}^+(t_k)$  in a well-designed filter has to converge quickly to the actual state and stay near it. Many of variables used in the simulation have to be initialized to zero before being employed for the first time. The initial simulated parameters of the test-case spacecraft are:  $a$  (semi-major axis) = 2477116 m,  $e$  (orbit eccentricity) = 0.70215,  $i$  (orbit inclination) =  $63.5^\circ$ , and  $\Delta t$  (time step) = 4 seconds.

## 7. Results

The results of the simulation prove that designing satellite attitude determination and control of satellite with only two-axis magnetometer sensors is possible. Fig. 1 shows the satellite attitude over a period of one orbit for both actual and estimated satellite attitude along all three axes. In order to better analyse the results, a close-up view of a small snapshot of the roll axes is shown in Fig. 1d. However, the sensor observations are randomly spread due to the presence of noise, instead of falling on the true attitude as in the case of an ideal sensor. In this situation, a discrete Kalman filter produces the optimal attitude estimation. The results demonstrate effective attitude tracking using the Kalman filter as it cuts through the noise. With using the filter, the range of measurements being  $9.3337 \times 10^{-5}$  degree is reduced to  $1.8786 \times 10^{-5}$  degree, so that it can help to control system more smoothly. The filter is also able to decrease the measurement standard deviation from  $1.5383 \times 10^{-3}$  degree to the estimation standard deviation of  $3.8888 \times 10^{-4}$  degree.

Figure 2 shows the satellite attitude rate estimation. The relation between the body rate, the angular rate and the orbital rate is given by (2), (3) and (4). The roll, pitch and yaw angles are derived from the angular rate what can be seen by comparing Fig. 1 and Fig. 2. Mostly these rates come from the rate gyroscopes but as shown, the estimated rates based on magnetometer measurements are accurate. Since magnetometers can only measure angles, no observations are shown in this figure.

Figure 3 shows control torques applied to the reaction wheels over a period of one satellite orbit. For this purpose, the output of the discrete Kalman filter served as the input to the controller. Comparing Fig. 2a with Fig. 2c, and Fig. 3a with Fig. 3c, the torques from the reaction wheels are opposing the roll rate and yaw rate in order to stabilize along both axes. However, the pitch axis behaves slightly different, as in (2). The cross-coupling effect and stiffness in the pitch axis produces a higher rate which can be seen in Fig. 2b.

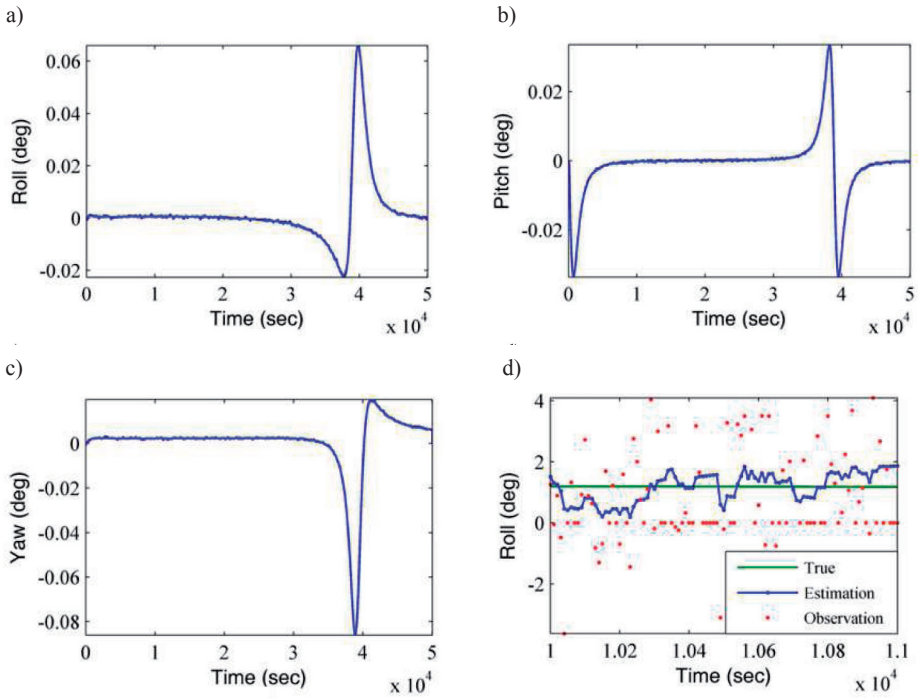


Fig. 1. The true and estimated response of satellite attitude: a) roll; b) pitch; c) yaw; d) roll snapshot.

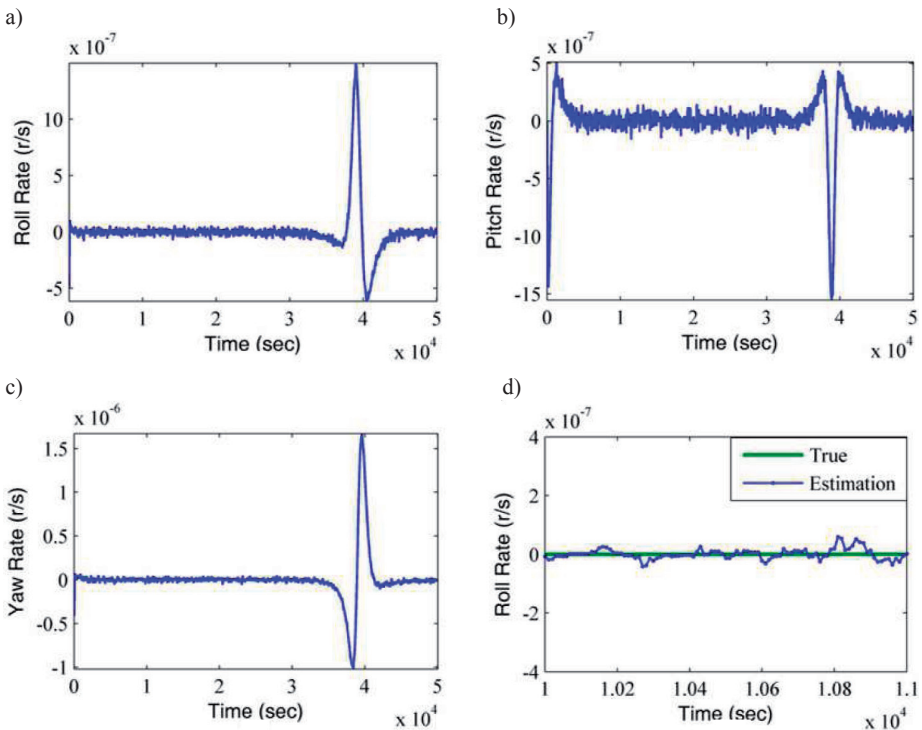


Fig. 2. The true and estimated satellite rate: a) roll; b) pitch; c) yaw; d) roll snapshot.

The reaction wheel torques are increased because of the cross-coupling of the reaction wheel momentum. This happens due to the attitude error along the axis. The reaction wheels turn against the angular momentum associated with spinning of the satellite around its own centre of mass until the satellite achieves the correct attitude.

As expected, at the perigee of orbit a bigger torque is applied to the pitch reaction wheel and therefore at the perigee the angular momentum of the pitch reaction wheel is also higher, as shown in Fig. 4.

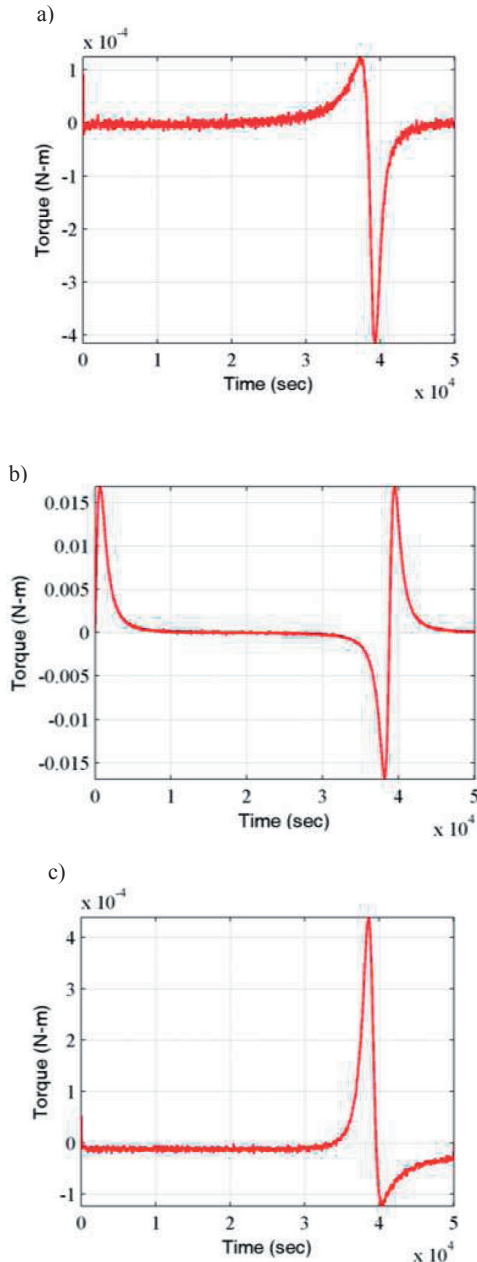


Fig. 3. The satellite control torque: a) roll; b) pitch; c) yaw.

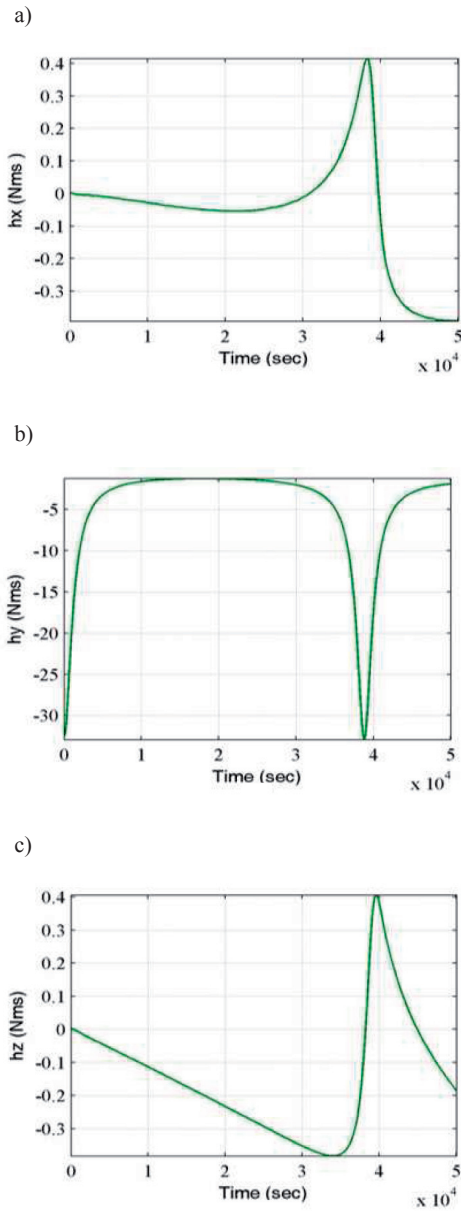


Fig. 4. The reaction wheel momentum: a) roll; b) pitch; c) yaw.

## 8. Conclusion

In this work, the satellite was modelled as a rigid body and satellite dynamics equations were derived and transformed into a state space equation and discretized, resulting in a difference equation. This difference equation is a plant model and consists of a state transition matrix and a deterministic control matrix. A two-axis magnetometer provided measurements to the Kalman filter and the filter output was fed into the controller to counteract disturbance torques. From the simulation results it was proved that the designed

three-axis estimation method based on only two-axis magnetometer is effective for predicting the satellite attitude from noisy sensor data. A filter designed in this work is coupled with the magnetometer and can reach the data standard deviation of  $3.8888 \times 10^{-6}$  degree which is an acceptable accuracy in space missions. Based on the results, the method for satellite attitude estimation using only two-axis magnetometer observations for attitude updates is feasible when the rate gyroscope sensor fails in the mission.

## References

- [1] Habib, T.M.A. (2013). A comparative study of spacecraft attitude determination and estimation algorithms (a cost-benefit approach). *Aerospace Science and Technology*, 26(1), 211–215.
- [2] Boardman, T.J. (1979). Prediction and Improved Estimation in Linear Models. *Technomet.*, 21(4), 582–582.
- [3] Lefferts, E.J., Markley, F.L., Shuster, M.D. (1982). Kalman filtering for spacecraft attitude estimation. *Journal of Guidance, Control, and Dynamics*, 5(5), 417–429.
- [4] Wertz, J.R. (1978). Spacecraft attitude determination and control. *Springer Scien. & Busin. Media*. 73, 858.
- [5] Wahba, G. (1965). A least squares estimate of satellite attitude. *SIAM review*, 7(3), 409–409.
- [6] Shuster, M.D. (2006). The quest for better attitudes. *Journal of the Astronautical Sciences*, 54(3–4), 657–683.
- [7] Markley, F.L. (1988). Attitude determination using vector observations and the singular value decomposition. *Journal of the Astronautical Sciences*, 36(3), 245–258.
- [8] Santoni, F., Bolotti, F. (200 0). Attitude determination of small spinning spacecraft using three axis magnetometer and solar panels data. *Aerospace Conference Proc., 2000 IEEE*, 7, 127–133.
- [9] Markley, F.L. (1993). Attitude determination using vector observations. *A fast optimal matrix algorithm*. 41, 261–80.
- [10] Faragher, R. (2012). Understanding the basis of the Kalman filter via a simple and intuitive derivation. *IEEE Signal processing magazine*, 29(5), 128–132.
- [11] Gelb, A. (ed.). (1974). Applied optimal estimation. *MIT press*, 374.
- [12] Ma, G.F., Jiang, X.Y. (2005). Unscented Kalman filter for spacecraft attitude estimation and calibration using magnetometer measurements. *Machine Learning and Cybernetics. Proc. Intern. Conf.*, 1, 506–511.
- [13] Psiaki, M.L., Martel, F., Pal, P.K. (1990). Three-axis attitude determination via Kalman filtering of magnetometer data. *Journal of Guidance, Control and Dynamics*, 13(3), 506–514.
- [14] De Ruiter, A. (2010). A simple suboptimal Kalman filter implementation for a gyro-corrected satellite attitude determination system. *Proc. Inst. Mech. Eng., Part G: Journal Aerospace Engineering*, 224(7), 787–802.
- [15] Sidi, M.J. (1997). *Spacecraft dynamics and control: a practical engineering approach*. Cambridge University Press.
- [16] Bolandi, H., Abedi, M., Nasrollahi, S. (2013). Design of an analytical fault tolerant attitude determination system using Euler angles and rotation matrices for a three-axis satellite. *Proc. Inst. Mech. Eng., Part G: Journal of Aerospace Engineering*, 0954410013479068.
- [17] Brown, R., Hwang, P.Y. (1996). *Introduction to Random Signals and Applied Kalman Filtering with Matlab Exercises and Solutions*. Wiley.
- [18] Anderson, J.L., Anderson, S.L. (1999). A Monte Carlo implementation of the nonlinear filtering problem to produce ensemble assimilations and forecasts. *Monthly Weather Review*, 127(12), 2741–2758.
- [19] Van der Merwe, R., Wan, E. (2003). Gaussian mixture sigma-point particle filters for sequential probabilistic inference in dynamic state-space models. *Acoustics, Speech, and Signal Processing. (ICASSP'03)*, 6, VI–701.
- [20] Julier, S.J., Uhlmann, J.K. (2004). Unscented filtering and nonlinear estimation. *Proc. IEEE*, 92(3), 401–422.
- [21] Arulampalam, M.S., Maskell, S., Gordon, N., Clapp, T. (2002). A tutorial on particle filters for online nonlinear/non-Gaussian Bayesian tracking. *Signal Processing. IEEE Transactions on*, 50(2), 174–188.

- [22] Shou, H.N., Lin, C.T. (2010, May). Micro-satellite attitude determination: using Kalman filtering of magnetometer data approach. *Computer Communication Control and Automation*, 195–198.
- [23] World Magnetic Model, NGIA, <http://www.ngdc.noaa.gov/geomag/WMM/DoDWMM.shtml>
- [24] Ogata, K. (1997). *Modern Control Engineering*. 299–231.